Migration of an asymmetric dimer in oscillatory fluid flow

H. S. Wright, Michael R. Swift, and P. J. King
School of Physics and Astronomy, University of Nottingham, Nottingham, NG7 2RD, United Kingdom
(Received 27 June 2007; revised manuscript received 15 July 2008; published 15 September 2008)

We describe the motion of an asymmetric dimer across a horizontal surface when exposed to an oscillatory fluid flow. The dimer consists of two spheres of distinct sizes, rigidly attached to each other. The dimer is found to move in a direction perpendicular to the fluid flow, with the smaller sphere foremost. We have determined how the speed depends upon the vibratory conditions, on the fluid viscosity, and on the dimer size and aspect ratio. Computer simulations are used to give an insight into the mechanism responsible for the motion. We use a scaling argument based on the asymmetry of the streaming flow to predict the approximate dependence of the migration speed on the system parameters.

DOI: 10.1103/PhysRevE.78.036311 PACS number(s): 47.55.Kf, 47.57.ef

I. INTRODUCTION

There is much current interest in the dynamics of fluid-particle systems. Examples of such systems include shear-induced ordering in colloidal suspensions [1,2], fluid-driven granular segregation [3], sand patterning on the sea bed [4], the motion of underwater cobbles [5], and swimming microstructures [6]. In addition to their fundamental scientific interest, very many of these phenomena are of technological importance.

One focus has been on neutrally buoyant particles suspended in liquids. In order to generate particle motion relative to the liquid, shear must be imposed on such a system. In many cases this gives rise to shear-induced migration in which the particles move through the fluid in response to the shear [2]. Recently there has been interest in non-neutrally-buoyant particles in viscous liquids [7]. Under oscillatory flows, spherical particles may form patterns and exhibit collective behavior [8,9]. Migration of spheres has also been observed in oscillatory flows close to a boundary [10]. The mechanisms responsible for many of these effects are not yet fully understood.

There is also considerable interest in the dynamics of nonspherical objects [11]. Collections of nonspherical particles exhibit collective dynamical behavior due to shape effects [12]. The simpler case of a single, nonspherical particle subjected to vertical vibration also exhibits nontrivial dynamical behavior [13]; a dimer will migrate across a vertically vibrated surface due to the coupling between rotation and friction. In all these cases, the presence of an ambient fluid is not required to generate motion.

In this paper we consider the influence of oscillatory fluid flow upon a single asymmetric object consisting of a pair of non-neutrally-buoyant spheres of unequal size glued together to form a dimer. We observe that, under horizontal vibration, such a dimer orients itself perpendicular to the flow and migrates across the lower surface of the cell in the direction of the smaller sphere. We have measured the dependence of the migration speed on vibratory conditions, fluid viscosity, and dimer size and aspect ratio. Computer simulations have been used to help understand the basic mechanism responsible for the motion. We show that the propulsion results from asymmetry in the streaming flow, and we provide a scaling argument to predict the dependence of the migration speed on system parameters. The migration of asymmetric objects in oscillating flows provides a new method for particle separation based on both size and shape [14] and may have many technological applications within microfluidic devices [15].

II. EXPERIMENTAL RESULTS

The dimers consist of two touching spheres held together by epoxy resin glue. In the majority of experiments, the spheres were made of stainless steel of density 7950 kg m^{-3}. We report here measurements on dimers of different sizes and for a range of size ratios between the smaller and larger spheres. However, in most of the experiments, the diameter of the larger sphere, d, was 2 mm and the diameter of the smaller sphere, d_s, was 1 mm. As will be discussed below, the migration speed is somewhat dependent on the quantity of glue used, characterized by the ratio G of the diameter of the glue-filled neck to d_s.

The dimers were vibrated within a liquid-filled cell formed by two horizontal 3-mm-thick glass sheets, each set into an aluminum alloy frame. The two frames were separated by a butyl rubber gasket to form a liquid-tight cell 136 mm long and 105 mm wide. The migration speed was found to be independent of the spacing between the glass sheets, provided it was at least $\simeq 3d/2$. The cell was mounted between two long-throw loudspeakers so that the plane of the glass sheets was accurately horizontal and only one-dimensional motion of the cell in the horizontal plane occurred. The sinusoidal motion may be characterized by the dimensionless acceleration of the cell, $\Gamma = A\omega^2/g$, determined using a capacitance acceleration sensor. Here A is the amplitude of the cell vibration, $\omega = 2\pi f$ is the angular frequency, and g is the gravitational acceleration. We used frequencies f in the range 20–50 Hz and Γ in the range 2–8.

The cell was filled with a water-glycerol mixture which had been vacuum pumped just prior to each experiment to remove dissolved air. This ensured that no air bubbles formed in the cell under vibration. The kinematic viscosity of the liquid, ν, was selected to be in the range 10^{-6}–10^{-5} m^2 s^{-1} by varying the glycerol concentration. The corresponding fluid densities were in the range 1–1.15 kg m^{-3}. The cell temperature was controlled to

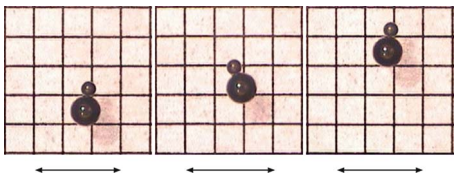

FIG. 1. (Color online) Movement of a 1:2 mm stainless steel dimer, immersed in a mixture of viscosity $\nu=2.0\times10^{-6}$ m^2 s^{-1}. The cell vibrates in the direction indicated by the arrowed lines, at 40 Hz and with $\Gamma=3.0$. The images were taken, from left to right, at 0, 2.7, and 6.7 s. The background grid has a 2 mm spacing.

±1 °C. A high-speed camera (up to 1000 frames/s) positioned above the cell was used both to observe the motion of the dimer in response to the vibration and to measure the slow dimer migration speed, perpendicular to the axis of vibration. In order to visualize the liquid flow patterns, a small amount of flow marker was sometimes added.

Initially, we will consider a stainless steel dimer made out of 1 and 2 mm spheres. Figure 1 shows the position of the dimer at three different times after vibration was established, as viewed from above the cell. As soon as vibration is applied, the dimer aligns itself perpendicular to the axis of vibration and begins to move in the direction of the smaller sphere. Because the spheres are *not* neutrally buoyant, their position with respect to the cell oscillates in the vibration direction at the driving frequency. The oscillation amplitude is somewhat different for the two spheres, as can be seen in Fig. 1. As a result the orientation of the dimer fluctuates by up to $\pm15°$ as it moves. If the orientation of the dimer in the horizontal plane is inverted, for example, in a collision with the cell boundary, the dimer will migrate back across the cell in the opposite direction, with the smaller sphere foremost. During their motion both spheres appear to remain in contact with the lower surface of the cell. In experiments with unpumped liquids, small air bubbles formed on the surface of the spheres under vigorous vibration, which enabled us to observe that, under vibration, the spheres slip on the surface without appreciable rolling [9].

During each cycle, the dimer is observed to speed up and slow down in the direction of migration. To average out these fluctuations we film the motion over many cycles and calculate the mean migration speed S. Figure 2 shows S as a function of Γ for a range of frequencies and for two different-sized dimers. The speed is seen to increase rapidly with increased vibrational amplitude and to be greater for lower frequencies at fixed Γ. The speed is also lower for larger dimers and for higher viscosities.

As the dimer is not neutrally buoyant, it rests on the lower surface of the cell and will be influenced by fluid drag and surface friction. Under vibration, the dimer will oscillate in the direction of vibration relative to the surrounding liquid. To quantify this behavior, the relative motion of the dimer with respect to the liquid needs to be determined experimentally. Since the liquid is incompressible, the liquid far from the dimer moves with the cell. The relative motion of the dimer with respect to the cell, and therefore relative to the distant liquid, was obtained from camera images. For convenience we determined the relative amplitude of motion of the

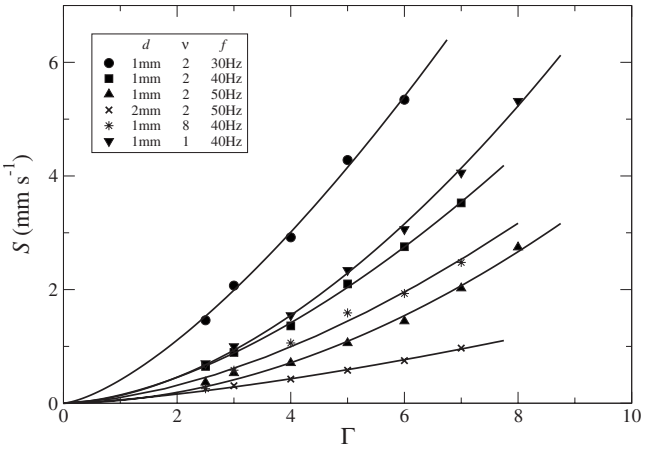

FIG. 2. Migration speed of stainless steel dimers with $G=0.42$ as a function of Γ. The viscosities given are in units of 10^{-6} m^2 s^{-1}.

larger sphere, A_r; this amplitude is also very close to the amplitude of motion of the center of mass of the dimer. Note that A_r will, in general, be different from A, as the spheres are moving in response to the fluid drag and surface friction [9,16]. Typically, A_r is approximately $A/2$. We have measured A_r and S for a range of oscillatory parameters, fluid viscosities, and particle sizes.

We have found it possible to collapse the data by displaying it in terms of two dimensionless numbers $A_r^2\omega/\nu$, and Sd/ν, appropriate to the motion in the two orthogonal directions. Figure 3 shows data for dimers with $G=0.42\pm0.02$, collapsed in this way. With the exception of the data points at the lowest values of $A_r^2\omega/\nu$, the data exhibit near linear behavior on the logarithmic plot shown, the gradient of the best-fit line being 0.82 ± 0.05.

Figure 4 shows the effect of changing the size ratio between the small and large spheres. The data can be collapsed by plotting $A_r^2\omega/\nu$ against SdR/ν, where R is the ratio of the

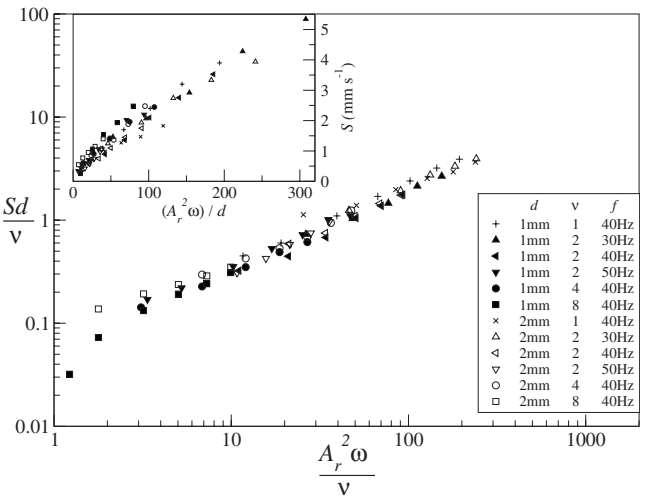

FIG. 3. Data for the migration speed of stainless steel dimers with $G=0.42$ as a function of the vibrational parameters, plotted in the form Sd/ν versus $A_r^2\omega/\nu$. The viscosities in the legend are in units of 10^{-6} m^2 s^{-1}. The inset shows, on a linear scale, that $S\sim A_r^2\omega/d$.

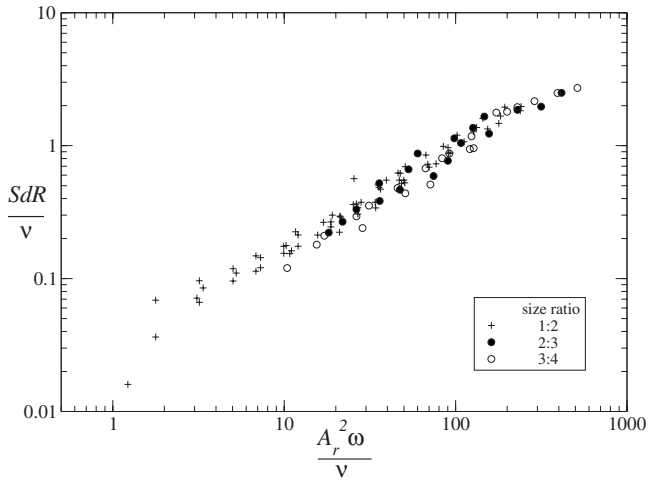

FIG. 4. Data for the migration speed of dimers made from stainless steel spheres with different sizes, plotted in the form SdR/ν versus $A_r^2\omega/\nu$. The data collapse is for a range of frequencies (30–50 Hz) and for the viscosities given in Fig. 3.

small- to the large-sphere diameter. In this figure the R values shown are 1/2, 2/3, and 3/4. The migration speed is seen to depend quite strongly on the asymmetry of the dimer. However, this simple dependence of S on R cannot persist for all values of R $(0 \leqslant R \leqslant 1)$, as a single sphere $(R=0)$ or a symmetric dimer $(R=1)$ is not observed to migrate. Indeed, we have carried out some experiments with $R=1/3$ and find that the fluctuations in the orientation of the dimer are so large that the migration speed is barely measurable.

We have also obtained data for dimers of different sizes (1:2 mm and 0.5:1 mm), each with $G=0.81\pm0.02$ and 0.34 ± 0.02. Each set of data scales in a similar way to that of Fig. 3, the data collapsing onto a straight line with a slope close to 0.8. However, the best-fit line for $G=0.81$ lies 35% higher in Sd/ν than the line for $G=0.42$. The best-fit line for $G=0.34$ lies 10% lower than the line for $G=0.42$. The dependency of S on the aspect ratio and on G shows that the migration speed is sensitive to the details of the shape of the object.

Finally, we note that the motion results from the asymmetry of the object coupled to the oscillatory fluid flow. The dimer does not migrate under horizontal vibration in the absence of the fluid, in contrast to the case where the vibration is vertical [13].

III. NUMERICAL SIMULATIONS

To aid our understanding of the mechanism responsible for generating the motion, we have carried out numerical simulations of the fluid-particle system. We have used a method based on the work of Kalthoff *et al.* in which the particles are represented by a fluid template [17]. The fluid is described by the three-dimensional incompressible Navier-Stokes equations

$$\frac{\partial \mathbf{v}}{\partial t} + (\mathbf{v}\cdot\nabla)\mathbf{v} = -\frac{1}{\rho}\nabla P + \nu\nabla^2\mathbf{v} - \mathbf{g}, \tag{1}$$

$$\nabla\cdot\mathbf{v} = 0. \tag{2}$$

Here $\mathbf{v}$ is the fluid velocity, P is the fluid pressure, ρ is the fluid density, and $\mathbf{g}$ is the acceleration due to gravity. These equations are discretized on a staggered marker and cell mesh [18] and solved using the projection method [19].

The dimer is treated as a solid object made out of two coupled spheres immersed in the fluid. The interaction between the dimer and fluid is achieved by representing the dimer as fluid moving with the instantaneous dimer velocity. This ensures that the no-slip boundary condition is enforced on the surface of the dimer. At each time step, the dimer's velocity is transferred to the fluid at the sites occupied by the dimer and the fluid evolves under the Navier-Stokes equations. The force on the dimer, $\mathbf{F}$, is then calculated from

$$\mathbf{F} = \sum_i (-\nabla P + \nu\rho\nabla^2\mathbf{v}), \tag{3}$$

where the sum is over all fluid sites occupied by the dimer. The derivatives in Eq. (3) are calculated using finite-difference approximations. This force is then used to update the dimer's position using molecular dynamics techniques [20]. This method has been used successfully to investigate the interaction between spheres in oscillatory flows [16].

In our simulations we consider a dimer with two touching steel spheres of diameters 1 and 2 mm; G is zero. The dimer moves in a liquid-filled cell of size 20×20 mm^2 in the horizontal plane and of depth 3 mm in the vertical direction. The simulation grid spacing is 0.1 mm in all three directions and a time step of 1×10^{-5} s is used throughout. The dimer moves under the influence of gravity and the oscillatory motion of the liquid. To avoid the complications associated with lubrication forces, the dimer is prevented from reaching the outer cells of the fluid grid by a contact force which restrains it to be at least two lattice spacings above the true cell boundary. The dimer is initially positioned horizontally at rest in the centre of the box. It falls under gravity until both spheres come into contact with the "surface." Under vibration, the dimer is observed to align perpendicular to the direction of oscillation and to move in the direction of the smaller sphere, as in the experiment.

Figure 5 shows dimer migration speeds obtained from simulation, scaled in the same way as the experimental data. Again the data collapse over a wide range of parameter values. The collapses in Figs. 3 and 5 are approximately linear on a log-log scale. While the experimental and simulated data have the same gradient at higher values of $A_r^2\omega/\nu$, the mean slope of the simulation data is somewhat higher than that of the experimental curve, having a gradient of $\approx1.2\pm0.1$. We believe that this discrepancy is due to discretization errors and to the simplified way we have treated the particle-surface interaction.

In our simulations we have ignored the frictional interaction between the dimer and the lower surface of the container. A rough estimate of the relative strength of frictional forces to drag forces for a steel particle in a steady flow of Reynolds number 100 suggests that frictional effects are an order of magnitude smaller than drag effects [21]. However, this estimate ignores the presence of the surface and the os-

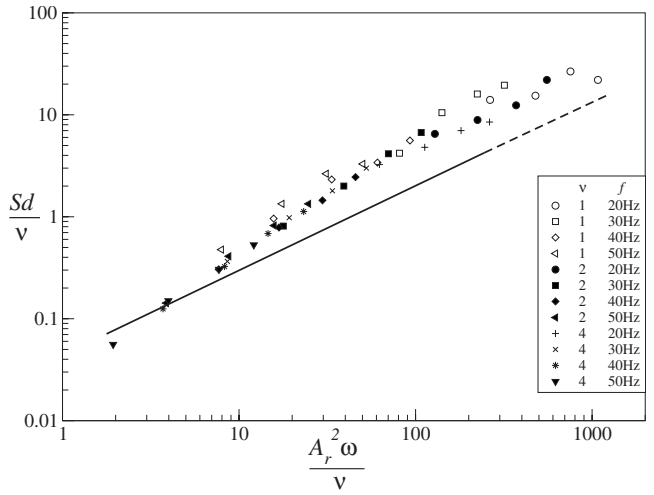

FIG. 5. Data obtained from simulation that have been scaled in the same way as the experimental data of Fig. 3. For comparison, the line shows a best fit to the experimental data. Again the viscosities given are in units of 10^{-6} m^2 s^{-1}.

cillatory nature of the flow. To investigate the importance of surface friction in our system, we have compared the relative amplitudes obtained from simulation, in which friction is absent, to the corresponding experimental values. These data are shown in Fig. 6. The simulated data are about 10% higher, which is consistent with our rough estimate of frictional effects.

We have also carried out some experiments in which we use a dimer made of glass spheres, having a density of 2500 kg m^{-3}. The migration speed lies between that of a steel dimer with the same size and aspect ratio and the corresponding simulation, for a given relative amplitude. This is consistent with frictional effects weakening as the mass of the dimer is reduced. It should be noted that, in simulation, the density of the dimer has no effect on the migration speed, provided the relative amplitude induced by the vibration of the container is the same.

In an attempt to obtain a closer agreement between simulation and experiment, we have carried out some simulations

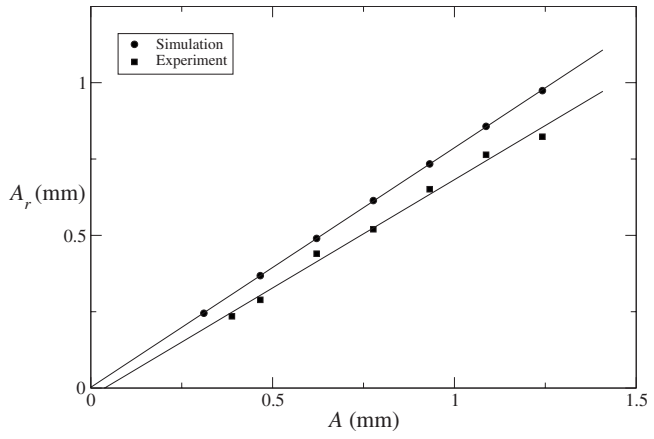

FIG. 6. Comparison between the applied vibrational amplitude A and the relative amplitude A_r obtained in simulations and from experiment. The dimer was of size 1:2 mm and vibrated at 40 Hz in a liquid of viscosity 2×10^{-6} m^2 s^{-1}.

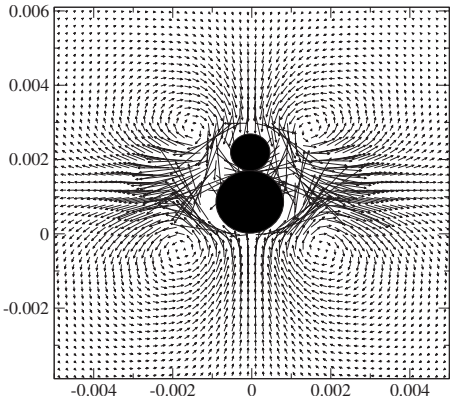

FIG. 7. Time-averaged velocity field around a 1:2 mm dimer vibrated in a fluid with $\nu=2\times10^{-6}$ m^2 s^{-1} at 50 Hz and with $\Gamma=5.0$. The vibration is from right to left. The flow shown occurs within a horizontal plane halfway up the smaller sphere. The dimensions given are in meters. The velocity at $x=0.0$, $y=-0.002$ has magnitude 2.0 mm s^{-1}.

in which we have included a *constant* Coulomb friction force with the lower surface. If the strength of the friction coefficient is chosen so that the relative amplitude agrees with the experimental value, the migration speed is found to be much lower than in experiment. Also, the simulated data no longer collapse in the same way as the experimental data. The frictional interaction of a single sphere with a surface in an oscillating liquid is known to have a complicated dependence on fluid and vibratory conditions [9]. Consequently, a more detailed investigation into the effects of surface friction on a dimer in the presence of an oscillating liquid is still needed. However, while friction influences the migration speed quantitatively, it is not the principal cause of the dimer's motion.

The reasonably good agreement between the simulations and experiment suggests that the simulation method is able to capture the dominant behavior of the fluid and may be used to provide information on the underlying propulsion mechanism.

At the Reynolds numbers used here, the fluid flow has a strong steady-streaming component [22]. The simulations can be used to obtain this streaming flow; an example is shown in Fig. 7. There is steady flow away from the dimer perpendicular to the dimer axis and an inflow along the axis. Similar flow patterns are observed in experiment using flow tracers. The outer streaming flow is similar to that observed for a single sphere, with four outer vortices [16,22]. However, in response to the asymmetry of the dimer, the time-averaged velocity field is also asymmetric. It is this asymmetry which drives the motion of the dimer.

Figure 3 showed an experimental data collapse having a gradient slightly less than unity, whereas the corresponding collapse from simulation, Fig. 5, displays a mean gradient slightly greater than unity. Were the gradient to be exactly unity, the migration speed of the asymmetric dimer would have the form $S\sim A_r^2\omega/d$ with no dependence on the fluid viscosity. The experimental data plotted in this way is shown in the inset to Fig. 3.

IV. DISCUSSION

To understand the motion of the asymmetric dimer, we consider the flow around an individual sphere. When the magnitude of an oscillatory flow varies along a solid surface, a steady secondary flow is generated [22]. The oscillatory flow around a sphere, outside a boundary layer with approximate thickness $\delta_{\mathrm{osc}}=\sqrt{2\nu/\omega}$, is well approximated as a potential flow. In our experiments this thickness is much less than the spheres diameters. It is known that, for a sphere, the steady flow velocity beyond the edge of the boundary layer scales as $u_s \sim A_r^2 \omega/d$ [23]. This steady flow velocity is independent of viscosity. Since both the experiments and simulations show that the dimer speed is also very weakly dependent upon fluid viscosity, it is plausible that the dimer speed is principally controlled by streaming flow.

Each sphere of the dimer is subjected to an incoming flow along the dimer axis. Were the dimer to be restrained from moving in the axial direction, the asymmetry in the flows would result in a net force on the dimer. Indeed, this force is readily measurable in simulation, the corresponding flow being similar to that shown in Fig. 7. The incoming streaming speed at the boundary of the larger sphere is similar to that at the smaller sphere, but the area over which it acts is more restricted for the smaller sphere. The two vortices associated with the smaller sphere are closer together than those of the larger sphere. It is principally this asymmetry in the areas of the incoming flows which provides a net force.

If the dimer is unrestrained, it will move in response to this force in the direction of the smaller sphere. This forward motion will modify the streaming flow pattern in such a way as to increase the force in the direction opposing this motion and weaken the force driving the motion, until the two forces balance. A simple model that captures the dominant features of the motion may be constructed as follows. From conservation of fluid momentum, the force on the asymmetric dimer due to flow around the larger sphere will be approximately of the form $F_1 \sim K_1(u_1-S)^2$ in the direction of the motion of the dimer, and the corresponding force on the smaller sphere will be of the form $F_2 \sim K_2(u_2+S)^2$ in the direction opposing the motion of the dimer. In the above expressions, u_1 and u_2 are the on-axis incoming streaming speeds and K_1 and K_2 are constants containing the fluid density and geometrical factors to account for the effective area over which each flow acts. Due to the asymmetry, the effective areas are not equal. From simulation we note that $S < u_1, u_2$. Because the streaming speeds are much larger than the dimer speed, the axial motion is not in the Stokes regime and fluid drag can be ignored.

During steady motion the forces F_1 and F_2 must balance and the speed of the asymmetric dimer will then be of the form $S=(K_1^{1/2}u_1-K_2^{1/2}u_2)/(K_1^{1/2}+K_2^{1/2})$. It is reasonable to assume that the inflows around the asymmetric dimer scale in the same way as the flow around a sphere [24]. Consequently, S is predicted to scale as $A_r^2\omega/d$, a good first approximation to both the experimental measurements and the simulations.

The experimental collapse shows that the migration speed has a slightly more complicated dependence on the system parameters than this simple analysis suggests. This could be due to the dependence of the boundary layer on these parameters. We have noted some dependence of S upon G and the presence of a boundary layer would certainly change the effective value of G. It should also be noted that the streaming flow generated by a sphere exhibits different flow regimes depending upon the fluid and oscillatory parameters [22,23]. It would therefore be interesting to carry out experiments for a wider range of control parameters than are obtainable in our experiments, to explore dimer migration under different streaming flow regimes.

In summary, we have shown that an asymmetric dimer undergoes lateral motion when in oscillatory fluid flow. We have used a numerical simulation to understand the mechanism for the propulsion and have developed a simple scaling argument to predict the observed dependence of the speed on the system variables. The ability to manipulate nonspherical objects in this way is expected to have wide technological application within the particle processing and microfabrication industries.

ACKNOWLEDGMENTS

We are grateful to the Engineering and Physical Sciences Research Council for support.

[1] For a review, see J. Vermant and M. J. Solomon, J. Phys.: Condens. Matter **17**, R187 (2005).
[2] G. Segre and A. Silberberg, J. Fluid Mech. **14**, 115 (1962); **14**, 136 (1962); J. Feng and D. D. Joseph, *ibid.* **324**, 199 (1996).
[3] M. E. Möbius *et al.*, Nature (London) **414**, 270 (2001); N. Burtally, P. J. King, and M. R. Swift, Science **295**, 1877 (2002); N. Burtally *et al.*, Granular Matter **5**, 57 (2003).
[4] G. Rousseaux, Phys. Rev. E **74**, 066305 (2006); J. L. Hansen *et al.*, Nature (London) **410**, 324 (2001).
[5] S. I. Voropayev *et al.*, Ocean Eng. **30**, 1741 (2003).
[6] R. Dreyfus *et al.*, Nature (London) **437**, 862 (2005).
[7] J. Bec, M. Cencini, and R. Hillerbrand, Physica D **226**, 11 (2007).
[8] G. A. Voth *et al.*, Phys. Rev. Lett. **88**, 234301 (2002).
[9] R. Wunenburger, V. Carrier, and Y. Garrabos, Phys. Fluids **14**, 7 (2002).
[10] S. Hassan *et al.*, Int. J. Multiphase Flow **32**, 1037 (2006).
[11] D. L. Blair, T. Neicu, and A. Kudrolli, Phys. Rev. E **67**, 031303 (2003); J.-C. Tsai, F. Ye, J. Rodriguez, J. P. Gollub, and T. C. Lubensky, Phys. Rev. Lett. **94**, 214301 (2005); V. Narayan, N. Menon, and S. Ramaswamy, J. Stat. Mech.: Theory Exp. (2006) P01005; H. S. Wright, M. R. Swift, and P. J. King, Phys. Rev. E **74**, 061309 (2006).
[12] A. Kudrolli, G. Lumay, D. Volfson, and L. S. Tsimring, Phys. Rev. Lett. **100**, 058001 (2008).

[13] S. Dorbolo, D. Volfson, L. Tsimring, and A. Kudrolli, Phys. Rev. Lett. **95**, 044101 (2005).
[14] For a review, see A. Kudrolli, Rep. Prog. Phys. **67**, 209 (2004), and references therein.
[15] For a review, see T. Laurell, F. Petersson, and A. Nilsson, Chem. Soc. Rev. **36**, 492 (2007).
[16] D. Klotsa, M. R. Swift, R. M. Bowley, and P. J. King, Phys. Rev. E **76**, 056314 (2007).
[17] W. Kalthoff *et al.*, Int. J. Mod. Phys. C **7**, 543 (1996).
[18] F. H. Harlow and J. E. Welch, Phys. Fluids **8**, 2182 (1965).
[19] K. Höfler and S. Schwarzer, Phys. Rev. E **61**, 7146 (2000).
[20] M. P. Allen and D. J. Tildesley, *Computer Simulations of Liquids* (Clarendon Press, Oxford, 1987).
[21] B. S. Massey, *Mechanics of Fluids* (Chapman and Hall, London 1994).
[22] N. Riley, Annu. Rev. Fluid Mech. **33**, 43 (2001).
[23] G. K. Batchelor, *An Introduction to Fluid Dynamics* (Cambridge University Press, Cambridge, U.K., 1967).
[24] C. K. Kotas, M. Yoda, and P. H. Rogers, Exp. Fluids **42**, 111 (2007).